ELSEVIER

Catalysis Today 37 (1997) 59–68

CATALYSIS TODAY

^{31}P nuclear magnetic resonance by spin echo mapping: A new tool to approach the oxidation state in VPO catalysts

A. Tuel*, M.T. Sananes-Schulz[1], J.C. Volta

Institut de Recherches sur la Catalyse, CNRS, 2 avenue A. Einstein, 69626 Villeurbanne Cedex, France

Abstract

This article reviews the possibilities of ^{31}P-NMR by spin echo mapping to gain information on the physico-chemistry of vanadium phosphorus oxide catalysts, particularly on poorly crystallized materials for which the X-ray diffraction technique is unsuccessful.

Keywords: Vanadium phosphorus oxide; NMR, ^{31}P-; Spin echo mapping

1. Introduction

Vanadium phosphorus oxides (VPO) have received considerable interest over the last few years because of their particular properties in the catalytic oxidation of *n*-butane into maleic anhydride [1–9]. Numerous VPO phases have been reported, with various structures and vanadium atoms in different oxidation states, and most of the active catalysts are actually mixtures of phases with different oxidation states and P/V ratios [10,11]. In particular, the V^{4+}/V^{5+} ratios seem to be critical for the catalytic performance of the material [12]. Therefore, it appears that the knowledge of the oxidation state of vanadium has been attempted by several groups using EPR spectroscopy or XPS [2,13–15]. However, most of the EPR signals were broad and difficult to interpret. Moreover, XPS gave information only about surface of the catalyst where the V^{4+}/V^{5+} ratio significantly differs from that of the bulk. Finally, most of the phases formed during reaction are amorphous or poorly crystalline, which often makes X-ray diffraction unsuccessful.

Solid-state nuclear magnetic resonance (NMR) has also been used to characterize VPO catalysts. Whereas interesting information could be obtained by ^{31}P- and ^{51}V-NMR on $VOPO_4$ phases, phases containing V^{4+} centers like the pyrophosphate, $(VO)_2P_2O_7$, gave no NMR signal under conventional conditions. In fact, interactions between the unpaired electrons of V^{4+} and ^{31}P nuclei make that the signal is considerably broadened and shifted with respect to that of $VOPO_4$. Li et al. [16] were the first to show that such NMR signals could be observed using a spin echo mapping technique. On $VOPO_4$ samples treated in *n*-butane, they could distinguish between V^{4+} and V^{5+} phases, and their evolution in course of reaction.

The aim of the present paper is to review some applications of ^{31}P-NMR by spin echo mapping to the characterization of various VPO catalysts. We have focused our attention on the identification of the phases and their oxidation states, particularly in the

*Corresponding author.

[1]On leave from INCAPE, Santa Fé, Argentina.

PII S0920-5861(96)00255-6

case of poorly crystalline phases, where X-ray diffraction is unsuccessful.

2. Experimental

The preparation of the pure reference phases and of the vanadium phosphorus oxide catalysts has been described elsewhere [11,12,17,18].

All ^{31}P-NMR experiments were performed on a Bruker MSL 300 NMR spectrometer using a probehead, allowing measurements in the 120–390 K temperature range. The ^{31}P spin echo mapping spectra were recorded under static conditions using a 90°x-τ–180°y-τ (acquire) sequence. The 90° pulse was 4.2 μs and τ was 20 μs. For each sample, the irradiation frequency was varied in increments of 50 kHz above and below the ^{31}P resonance of H_3PO_4. The number of spectra thus recorded was dictated by the frequency limits beyond which no spectral intensity was visible. The ^{31}P-NMR information by spin echo mapping was then obtained by superposition of all individual spectra.

3. Results

3.1. ^{31}P-NMR spectra by spin echo mapping of reference phases

Various phases with different P/V ratios and oxidation states have been characterized by ^{31}P-NMR by spin echo mapping. For α_{II}-, β-, γ-and δ-$VOPO_4$, the NMR spectra by spin echo mapping consist of a single line at ~0 ppm [17]. Therefore, the technique does not permit the identification of the $VOPO_4$ phases, which can be done using conventional ^{31}P magic angle spinning (MAS) NMR [11].

In contrast, for V^{4+} phases, the position and shape of the NMR line are characteristic of the material. We have already reported that, for these phases, ^{31}P-NMR lines were in the 1500–2500 ppm range [17–19]. More precisely, the shift was 1625 ppm for the hemihydrate, $VOHPO_4{\cdot}0.5H_2O$, 2300 ppm for $VO(H_2PO_4)_2$ (phase E) and 2600 ppm for crystallized pyrophosphate $(VO)_2P_2O_7$ (Fig. 1). As will be discussed later, the observed shift depends on the interaction between the unpaired electron of V^{4+} species and the ^{31}P nuclei via an oxygen bridging, and is, therefore, characteristic of V–O–P units in the structure.

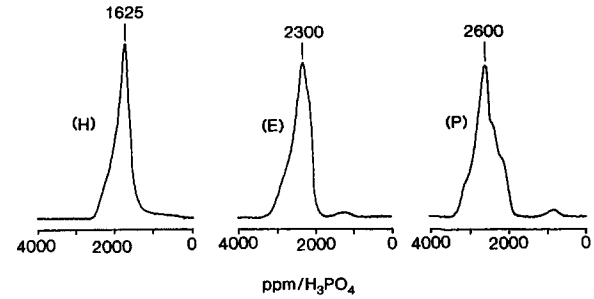

Fig. 1. ^{31}P-NMR spectra by spin echo mapping of (V^{4+}) VPO phases: H, hemihydrate; phase E, $VO(H_2PO_4)_2$; P, pyrophosphate. E and $(VO)_2P_2O_7$ were calcined for 100 h under nitrogen at 750°C.

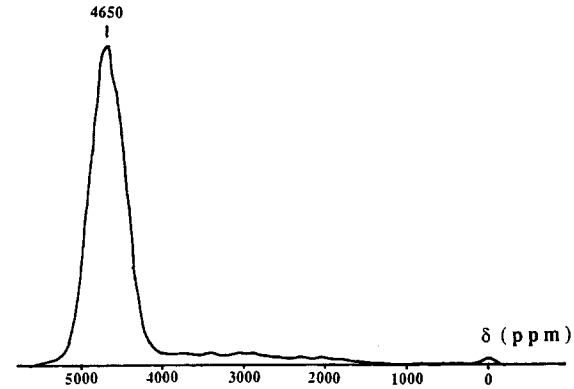

Fig. 2. ^{31}P-NMR spectrum by spin echo mapping of VPO_4 (V^{3+} phase).

Fig. 2 shows the ^{31}P-NMR spectrum by spin echo mapping of VPO_4 obtained by reduction of $(VO)_2P_2O_7$ under 5% H_2/Ar at 900°C [17]. A single, broad peak is observed at ~4650 ppm without any signal characteristic of V^{4+} phases in the 1500–2500 ppm range. Thus, such a shift can be unambiguously attributed to the presence of V^{3+} cations in VPO_4. Since V^{3+} cations have a $3d^2$ configuration, and since the ^{31}P-NMR shift is proportional to the electron–nuclear interaction, the NMR line is expected to be in the 3000–5000 ppm range for V^{3+} phases, which is observed experimentally.

The ^{31}P-NMR signal by spin echo mapping strongly depends on the purity of the phases. For the hemihydrate, $VOHPO_4{\cdot}0.5H_2O$, obtained after a short crystallization time (3 h of refluxing), an intense

shoulder is observed in the 250–1000 ppm range, which appears to be connected with the crystallinity of the sample since the XRD pattern of the material shows distinct relative intensities for the (001) and (220) reflections, as compared to a sample obtained after 16 h of refluxing (Fig. 3).

Calcination of the precursor $VOHPO_4{\cdot}0.5H_2O$ leads to the formation of the pyrophosphate phase, as evidenced by XRD. However, depending on the weight of the precursor in the reactor, different NMR spectra are observed (Fig. 4). For the lower weight, an additional line is observed at −150 ppm, characteristic of P atoms bonded to V^{4+} of the $VO(PO_3)_2$ matrix. In contrast, a line at 4650 ppm is observed in the spectrum of the sample obtained with the higher weight of the precursor, showing the presence of a V^{3+} phase. It is interesting to note that neither the V^{5+} phase nor the V^{3+} phase could be detected by XRD. Such experiments clearly demonstrate that an increase in the weight of precursor results in a reduction of the catalyst. Moreover, the increase in the line width in Fig. 4a and c as compared to Fig. 4b is in agreement with a loss in the crystallinity, as observed by XRD.

In a similar manner, calcination of the phase *E* leads to the formation of $VO(PO_3)_2$. When the phase *E* is calcined under N_2, poorly crystalline $VO(PO_3)_2$ is observed by XRD, in agreement with the broad NMR spectrum in Fig. 5a. Fig. 5 (b and c) corresponds to materials calcined under air for 4 and 20 h,

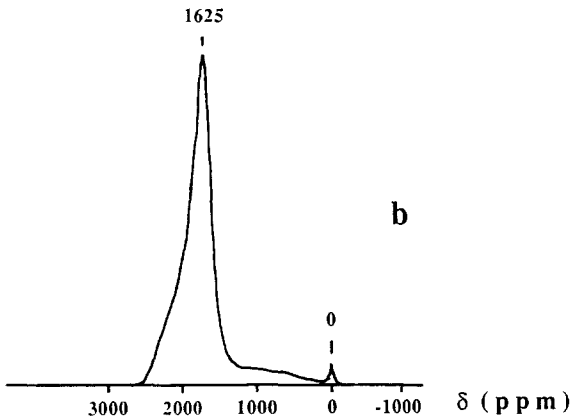

Fig. 3. Influence of time of refluxing of isobutanol on the ^{31}P-NMR spectra by spin echo mapping of $VOHPO_4{\cdot}0.5H_2O$: (a) 3 h and (b) 16 h.

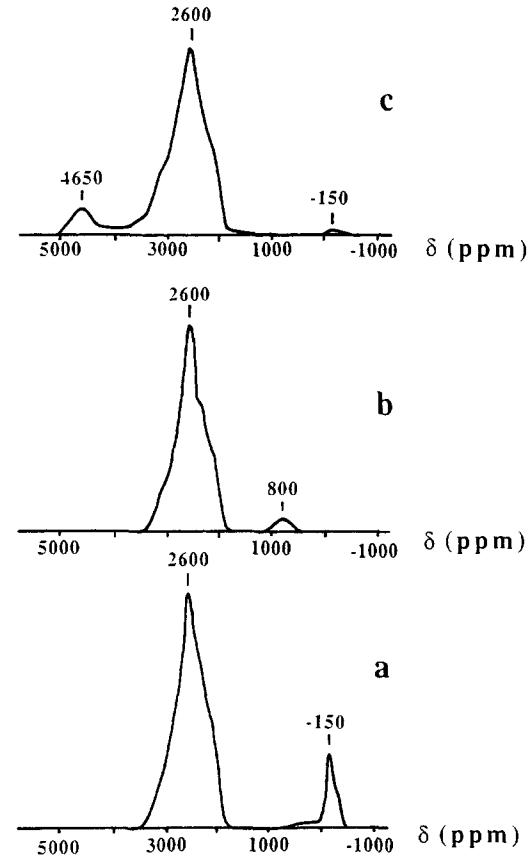

Fig. 4. Calcination of $VOHPO_4{\cdot}0.5H_2O$ at 750°C under nitrogen: influence of the mass of the precursor on the ^{31}P-NMR spectra by spin echo mapping of the VPO catalysts obtained: (a) 1.5 g, (b) 2.0 g and (c) 3.0 g.

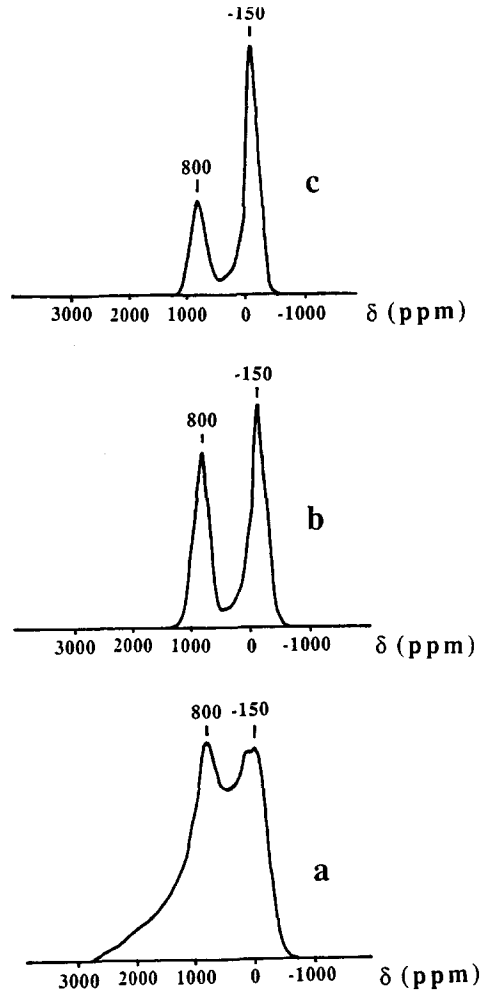

Fig. 5. Influence of the conditions of calcination at 500°C of $VO(H_2PO_4)_2$ on the ^{31}P-NMR by spin echo mapping spectra of the VPO catalysts obtained: (a) after 4 h under nitrogen, (b) after 4 h under air and (c) after 20 h under air.

respectively. $VO(PO_3)_2$ is still observed by XRD on both samples, with higher crystallinities as compared to the material calcined under N_2. For the three samples, the peak at ~800 ppm has been attributed to P atoms bonded to V^{4+} centers in $VO(PO_3)_2$, whereas the peak at −150 ppm was suggested to be due to P atoms bonded to V^{5+} in strong interaction with $VO(PO_3)_2$. The conditions of treatment as well as the duration of calcination influence the relative distribution of the peaks at 800 and −150 ppm. This emphasizes the interest of ^{31}P-NMR by spin echo mapping to reveal the change of the V^{4+} distribution with the conditions of treatment. It is not surprising to observe an increase in the V^{5+} contribution from N_2 because of air treatment and duration.

3.2. *Application to the study of the activation of a VPO precursor*

The spin echo mapping technique has been applied to monitor the evolution of a VPO catalyst in the *n*-butane oxidation reaction during the activation time. The hemihydrate phase, $VOHPO_4{\cdot}0.5H_2O$, was activated at 400°C in an *n*-butane–air mixture for different periods, e.g., 0.1, 8, 84 and 132 h. XRD showed that all samples were poorly crystallized, but revealed the presence of $(VO)_2P_2O_7$ reflections at 2θ=23°, 28.45° and 29.94° and also V^{5+} phases, particularly δ-$VOPO_4$ (reflections at 2θ=22.08°, 24.16° and 28.55°). Increasing the activation time shows an increase in the amount of $(VO)_2P_2O_7$ in the material, but a quantification of this amount in the various samples is quite impossible. The ^{31}P-NMR spectra by spin echo mapping (normalized with respect to the line at 0 ppm) of the four samples are shown in Fig. 6. All spectra show a peak at ~0 ppm, characteristic of V^{5+} phases, and a broad line at ~2400 ppm is attributed to a poorly crystallized pyrophosphate phase (note that for well crystallized pyrophosphate, this signal is observed at 2600 ppm, see Fig. 1). It is interesting to note that the hemihydrate phase, char-

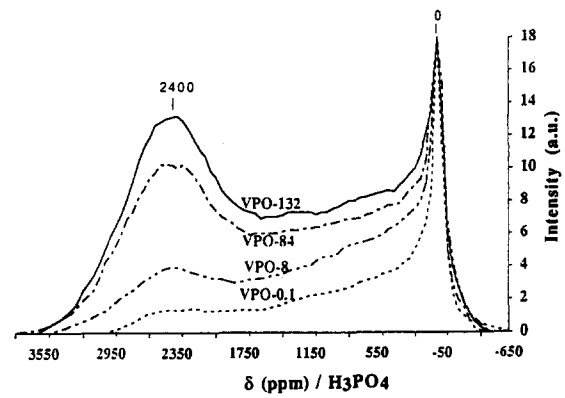

Fig. 6. Influence of the time of activation at 400°C under the catalytic atmosphere (nC_4H_{10}/O_2/He::1.6/18/80.4, VSHV=1500 h^{-1}) on the ^{31}P-NMR spectra by spin echo mapping spectra of the corresponding VPO catalysts.

acterized by an NMR line at 1625 ppm, has completely disappeared after 0.1 h in stream and that the corresponding sample contains essentially V^{5+} phases. In agreement with the XRD data, the relative area of the peak at 2400 ppm increases with the activation time. The peak is broad and slightly shifted as compared to that obtained on a pure, highly crystalline $(VO)_2P_2O_7$, which is a consequence of the low crystallinity of the sample. The broad signal in the 300–1500 ppm range, whose relative intensity also increases with the activation time, has been attributed to a disorganized material where mixed valence V^{4+}–V^{5+} pairs could be present. A quantitative estimation of the relative amounts of $(VO)_2P_2O_7$ and V^{5+} phases in the samples was performed by measuring the areas under the NMR lines at 2400 and 0 ppm, respectively. Thus, we could estimate that the percentage of V^{5+} phases in the samples decreased from 39% after 0.1 h of activation to 17% after 84 h of activation. For these samples, the conventional ^{31}P MAS NMR showed that V^{5+} phases were essentially composed of δ-$VOPO_4$ and α_{II}-$VOPO_4$.

Whereas the sample activated for 0.1 h contains only δ-$VOPO_4$, the sample activated for 132 h contains ~60% δ-$VOPO_4$ and 40% α_{II}-$VOPO_4$. Therefore, the change of the NMR spectra was attributed to a progressive transformation of δ-$VOPO_4$ into α_{II}-$VOPO_4$. The results of this study allowed us to propose a scheme for change of the catalyst with activation time (Fig. 7). First, the precursor, is partly transformed into $(VO)_2P_2O_7$ via a topotactic process and is partly oxidized into δ-$VOPO_4$. Both phases are very poorly crystallized at 400°C, but can be detected by ^{31}P-NMR by spin echo mapping. Upon activation time, δ-$VOPO_4$ is reduced to $(VO)_2P_2O_7$ and also transformed to α_{II}-$VOPO_4$, as was evidenced by in situ Laser Raman Spectroscopy [11].

3.3. *Application to the study of poorly crystallized materials*

Three precursors, P1, P2 and P3 (hemihydrate phase $VOHPO_4{\cdot}0.5H_2O$), were prepared following different recipes already reported [20]. These precursors were then activated under *n*-butane–air mixture for 75 h (1.5 cm^3 of precursor, T=385°C, GSHV=1000 h^{-1}). The ^{31}P-NMR spectra by spin echo mapping of the precursors are shown in Fig. 8. In all cases, an intense line at 1625 ppm, characteristic of PO_4 units bounded to V^{4+} cations in the hemihydrate phase, is observed. The higher intensity as well as the smaller line widths for P1 and P2 are in agreement with a higher degree of crystallinity of these materials as evidenced by XRD. The broad line in the 200–1200 ppm range, more intense for the less crystallized precursor P3, has already been attributed to the presence of V^{4+} cations in a disorganized environment. It is interesting to note that the ^{31}P-NMR signal by spin echo mapping is not sensitive to the difference in morphology among P1, P2 and P3, as observed by XRD and electron microscopy. Although ^{31}P-NMR spectra of the precursors are similar in shape, it is not the case for the activated catalysts (Fig. 9). C1 (corresponding to precursor P1) shows essentially one line at 0 ppm that can be unambiguously attributed to V^{5+} phases. C2 still shows V^{5+} phases together with a very broad line

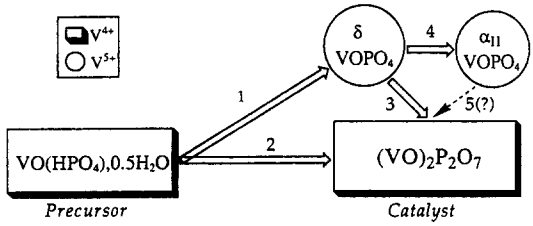

1: Oxydehydration
2:Topotactic transformation
3,5: Reduction V^{5+} to V^{4+}
4: Isovalence transformation

Fig. 7. Scheme of the proposed evolution of the VPO catalysts with time of activation [12].

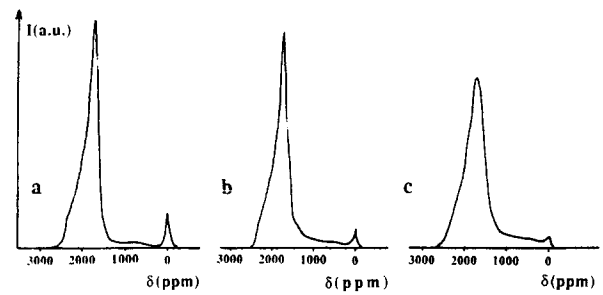

Fig. 8. Influence of the mode of preparation on the ^{31}P-NMR spectra by spin echo mapping of $VOHPO_4{\cdot}0.5H_2O$: (a) P1/aqueous route (HCl as the reducing agent of V_2O_5), (b) P2/Organic route (isobutanol as the reducing agent of V_2O_5) and (c) P3/Organic route (isobutanol as the reducing agent of $VOPO_4{\cdot}2H_2O$).

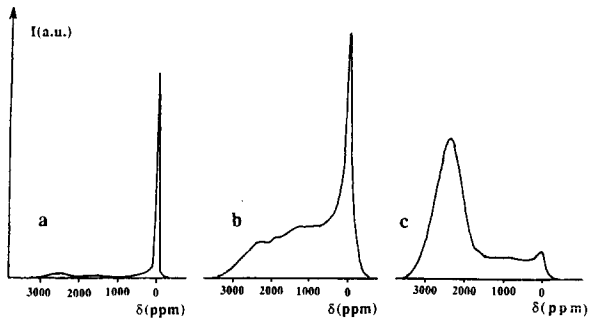

Fig. 9. ^{31}P-NMR spectra by spin echo mapping of VPO catalysts activated (385°C under 1.5% *n*C4/air, VSHV=100 h^{-1} for 75 h) from the $VOHPO_4 \cdot 0.5H_2O$ precursors presented in Fig. 8: (a) catalyst C1 (ex P1), (b) catalyst C2 (ex P2) and (c) catalyst C3 (ex P3).

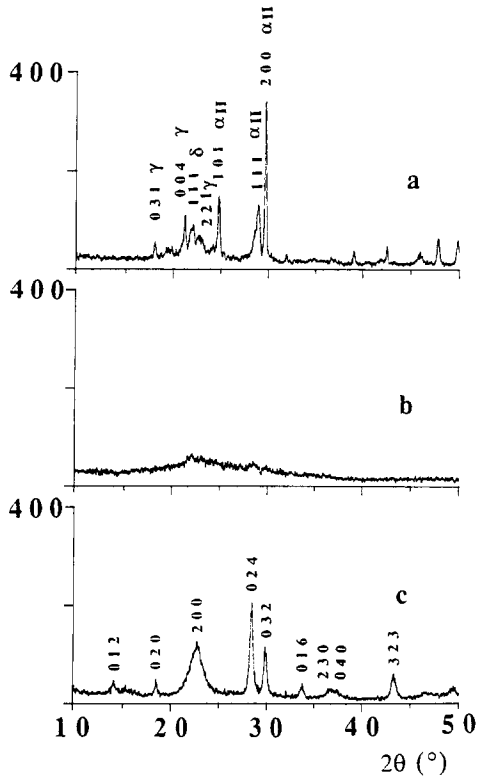

Fig. 10. XRD spectra of catalysts C1, C2 and C3: (a) catalyst C1 (ex P1), (b) catalyst C2 (ex P2) and (c) catalyst C3 (ex P3).

lying in the 500–3000 ppm range. As shown in Fig. 10, the material is totally amorphous as no peaks can be detected in the XRD pattern. On the basis of preliminary observations made on the reference phases, the presence of an NMR signal at ~2500 ppm can be attributed to $(VO)_2P_2O_7$, and the spectrum is consistent with a disorganized pyrophosphate structure supporting V^{5+} phases. In contrast, C3 shows an intense line at 2600 ppm assigned to crystalline $(VO)_2P_2O_7$, as revealed by XRD, together with disorganized $(VO)_2P_2O_7$. Catalytic data clearly confirmed that catalyst C3, consisting mainly of $(VO)_2P_2O_7$, is the most active and selective phase.

The main interest of ^{31}P-NMR by spin echo mapping thus stems in the possibility to detect low amounts of the $(VO)_2P_2O_7$ phase, particularly on poorly crystalline materials and to be able to discriminate between the crystalline $(VO)_2P_2O_7$ (peak at 2600 ppm) and a disorganized V^{4+} matrix, postulated with a broad signal in the 300–1500 ppm range. This appears highly important as the catalytic role of the amorphous phase has sometimes been considered as a key for the activity of the VPO catalysts. Another interesting observation is that the best catalytic results are obtained over a structure, for which P atoms are connected to both the V^{4+} ions in crystallized $(VO)_2P_2O_7$ and the V^{4+} cations in a disorganized matrix. This disorganized matrix could favor the re-oxidation of V^{4+} to V^{5+} and, thus, improve the catalytic activity in the mild oxidation of *n*-butane.

3.4. *Difference between 'equilibrated' and 'non-equilibrated' catalysts*

Thus far, no information has been reported on industrial VPO catalysts, as studied by ^{31}P-NMR by spin echo mapping. It is interesting to see if there is any difference in the spectra between 'equilibrated' catalysts (higher than 1000 h activation) and 'non-equilibrated' catalysts (lower time of activation). We present here results obtained on catalysts which belong to an earlier generation of a promoted vanadium phosphate catalyst obtained for commercial production. While details of its composition and manufacture cannot be disclosed, the general preparation procedures of such VPO catalysts consists of dissolution and reduction of V_2O_5 in anhydrous alcohol (isobutanol is generally preferred) by bubbling gaseous HCl through the solution at a temperature lower than 60°C, a further phosphoric acid addition and digestion under reflux and stripping of the alcohol [4]. This precursor was characteristic of the VOH-

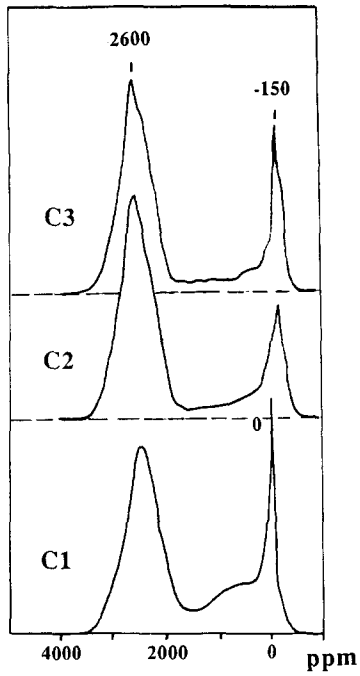

Fig. 11. ^{31}P-NMR spectra by spin echo mapping of industrial VPO catalysts activated for different periods: C1, after 100 h; C2, after 300 h; C3, after 720 h.

$PO_4{\cdot}0.5H_2O$ precursor with some residual $VO(H_2PO_4)_2$ phase (*E* phase).

Fig. 11 shows the ^{31}P-NMR spectra by spin echo mapping of the three catalysts. The signal observed at 2600 ppm corresponds to P atoms bonded to V^{4+} in the well-organized $(VO)_2P_2O_7$ matrix. This signal is observed for all the three catalysts. The intense signal observed near 0 ppm for C1 is characteristic of the $VOPO_4$ phases present on this catalyst as detected by XRD, while a peak at −150 ppm only is observed for C2 and C3. Note that the calcination of $VO(H_2PO_4)_2$ (phase *E*) under air gives two signals which are observed at 800 and −150 ppm and which have been previously attributed, respectively, to P atoms bonded to V^{4+} of the $VO(PO_3)_2$ matrix and to V^{5+} cations dispersed on the $VO(PO_3)_2$ matrix and for which the relative distribution favors the second one with the time of activation. The evolution of the spectra from C2 to C3 in the 1000 to −1000 ppm range shows an increase in the signal at −150 ppm. This signal is the fingerprint of a nucleated, oxidized $VO(PO_3)_2$ phase (V^{5+}/$VO(PO_3)_2$) coming from the activation of the residual *E* phase present on the $VOHPO_4{\cdot}0.5H_2O$ precursor. The large signal observed in the 300–1500 ppm for C1 corresponds to P atoms in a disorganized pyrophosphate structure, as was observed previously. It is noteworthy that this shoulder decreases with the time of activation from C1 to C3.

The main interest of ^{31}P-NMR by spin echo mapping in this study stems in the possibility to detect low amounts of residual phases in VPO materials which cannot be detected by X-ray diffraction.

3.5. *Application of ^{31}P-NMR by spin echo mapping to the preparation of the precursor*

^{31}P-NMR by spin echo mapping has been used as a complement to XRD to monitor the preparation of the precursor, $VOHPO_4{\cdot}0.5H_2O$, from reduction of $VOPO_4{\cdot}2H_2O$ with isobutanol, as seen in Fig. 12 [20]. Upon reduction, XRD shows that the lines characteristic of $VOPO_4{\cdot}2H_2O$ progressively decrease in intensity and are displaced with refluxing time, indicating a regular transformation of the hemihydrate phase. After 4 h, new lines appear at 2θ=15.65° and 30.4°, corresponding to $VOHPO_4{\cdot}0.5H_2O$. It is interesting to note the presence of weak peaks at 22.5° (after 2 h) and 21.5° (after 4 h) which could be due to an intermediate hydrated $VOPO_4$ phase.

The ^{31}P-NMR spectrum by spin mapping of $VOPO_4{\cdot}2H_2O$ shows a typical signal at 0 ppm, indicative of P atoms bonded to V^{5+} species in the structure. After 2 h of refluxing, we mainly observe the signal characteristic of $VOPO_4{\cdot}2H_2O$ at 0 ppm, but additional lines are present at 100 and 1625 ppm. The latter signal is indicative of the beginning of the appearance of $VOHPO_4{\cdot}0.5H_2O$, whereas the signal at 100 ppm could correspond to an intermediate hydrated $VOPO_4$ phase, as was postulated previously. This was confirmed by a conventional ^{31}P-NMR characterization under static conditions of the corresponding material: two signals were observed, which provided evidence for the existence of two different environments of P atoms in $VOPO_4$ structures. After 4 h, the line at 100 ppm has been displaced to ~600 ppm, showing that the intermediate hydrated phase has been modified. After 8 h, only signals at 1625 and 0 ppm are observed. The signal at 0 ppm almost disappears at 16 and 23 h. Data show that the transformation of $VOPO_4{\cdot}2H_2O$ into $VOHPO_4{\cdot}0.5H_2O$ is

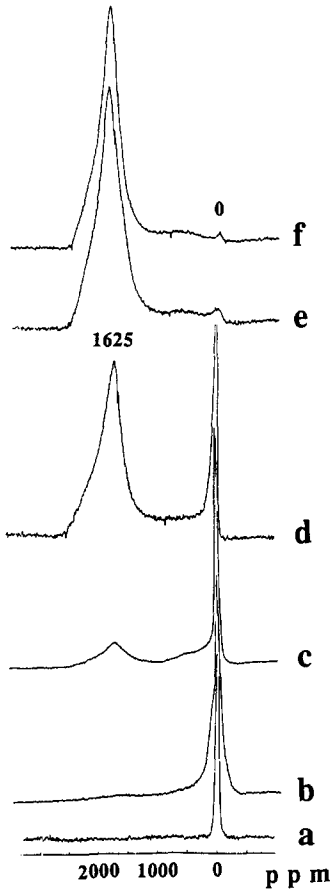

Fig. 12. Temporal evolution of the ^{31}P-NMR spectra by spin echo mapping spectra of the material obtained by refluxing $VOPO_4{\cdot}2H_2O$ with isobutanol: (a) starting $VOPO_4{\cdot}2H_2O$; (b), (c), (d), (e) and (f) after 2, 4, 8, 16 and 23 h of refluxing, respectively.

almost complete after 16 h of refluxing in isobutanol. The small contribution in the 300–1500 ppm range, which was previously attributed to the P atoms in the disorganized V^{4+} structure, progressively disappears with time, reflecting an increase in the crystallization of the hemihydrate.

In this way, ^{31}P-NMR by spin echo mapping has come out as a powerful technique that enables an improved understanding of the preparation of $VOHPO_4{\cdot}0.5H_2O$ from $VOPO_4{\cdot}2H_2O$. Intermediate hydrated $VOPO_4$ phases, difficult to observe by X-ray diffraction, could be detected by this method. Moreover, $VOHPO_4{\cdot}0.5H_2O$ was more easily detected by ^{31}P-NMR by spin echo mapping as compared to XRD.

3.6. *^{31}P-NMR by spin echo mapping at low temperature*

The frequency shift observed in ^{31}P-NMR by spin echo mapping on the V^{4+} or V^{3+} phases is related to the atomic susceptibility of the material, X_{at}, by

$$\delta = (H_{eff}/\beta) f X_{at} \quad (1)$$

where H_{eff} is the hyperfine field for phosphorus, β is the Bohr magneton and f is a fractional contribution of the unpaired electron spin of vanadium species to the ^{31}P nucleus.

X_{at} can be described by a Curie–Weiss law and, therefore, the frequency shift is a function of temperature:

$$\delta = C/(T - \theta) \quad (2)$$

where C is the Curie constant and θ is the Weiss temperature. Fig. 13 shows the evolution of ^{31}P-NMR spectra by spin echo mapping of the pyrophosphate

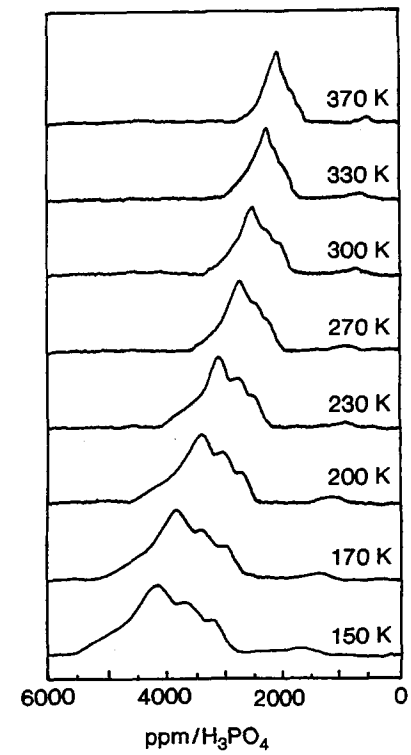

Fig. 13. Influence of temperature on the ^{31}P-NMR spectra by spin echo mapping of $(VO)_2P_2O_7$.

phase $(VO)_2P_2O_7$ with temperature. We observe that the frequency shift decreases with temperature from ~4200 ppm at 150 K to 2000 ppm at 370 K. In the working temperature range, the inverse frequency shift ($1/\delta$) is a linear function of temperature for both the hemihydrate and pyrophosphate phases, in agreement with Eq. (2). Extrapolation of the curves to $1/\chi=0$ gives an estimation of the Weiss temperature. For $VOHPO_4 \cdot 0.5H_2O$, we find $\theta=-25.3$ K, in very good agreement with the value obtained by direct measurement of the magnetic susceptibility. For $(VO)_2P_2O_7$, the value of δ was found to be ≈ -75 K, slightly different from that obtained by susceptibility measurements. However, a value of -65 K was found on a second pyrophosphate sample having a slightly lower crystallinity, and corresponding to the value obtained by direct measurement. The measurement of δ is quite difficult on $(VO)_2P_2O_7$ because of the line width, particularly at low temperatures. Indeed the spectrum is split into 4 lines, which is particularly evident at 150 K (Fig. 14). The lines are not due to different crystallographic environments in the structure, but due rather to variations in the oxidation state of vanadium atoms. Indeed, it has been reported that each pair of sharing octahedra in $(VO_2)P_2O_7$ could be considered as a redox system inside the crystalline matrix [10]. The real oxidation state of vanadium ions is not 4 but 3.69 and 4.19 for one of the pairs and 3.79 and 4.44 for the other. Therefore, the electron-spin density on each phosphorus atom depends on its location in the structure and may explain the presence of 4 lines in the ^{31}P-NMR spectrum.

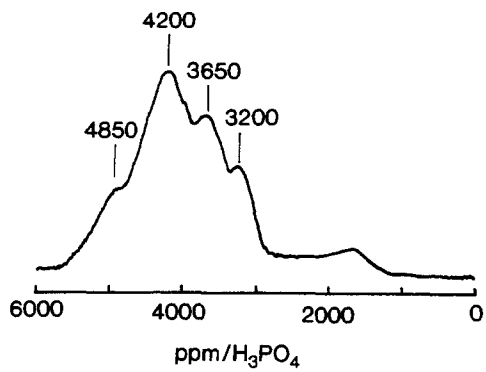

Fig. 14. ^{31}P-NMR spectrum by spin echo mapping of $(VO)_2P_2O_7$ at 150 K.

4. Conclusions

The various examples of application of ^{31}P-NMR by spin echo mapping for the characterization of VPO catalysts have shown the power of the method to obtain information on the structure of these materials. In particular, since the NMR shift on the ^{31}P line depends on the contribution of the unpaired electron spin to the ^{31}P nuclei, the ^{31}P-NMR spectrum by spin echo mapping immediately provides information about the different oxidation states of vanadium centers in the sample. Moreover, the position and the shape of the NMR line is structure-sensitive which makes possible the difference between phases with the same oxidation state, like $VOHPO_4 \cdot 0.5H_2O$, $VO(H_2PO_4)_2$, $(VO)_2P_2O_7$, $VO(PO_3)_2$ and amorphous V^{4+} containing matrix.

A great advantage of the technique is that it makes possible the characterization of poorly crystalline phases that do not show any signal by X-ray diffraction. It was particularly useful to study the evolution of a VPO catalyst during the activation time and to study the preparation of the precursor, $VOHPO_4 \cdot 0.5H_2O$, from a V^{5+} phase.

The technique can also be applied to the determination of the characteristics of VPO catalysts used for the oxidation of light alkanes like ethane, propane or *n*-pentane.

We have also shown that magnetic characteristics of pure phases like the Weiss temperature could be easily determined from variable temperature spin echo mapping spectra. Moreover, at low temperatures, the spectrum of $(VO)_2P_2O_7$ showed 4 lines, in agreement with four different oxidation states for vanadium atoms in the structure.

References

[1] G. Centi (Ed.), Vanadyl Pyrophosphate Catalysts, Catal. Today, Vol. 16, No. 1, Elsevier, Amsterdam, 1993.
[2] G. Centi, F. Trifiro, J.R. Ebner and V.M. Franchetti, Chem. Rev., 88 (1988) 55.
[3] C.A. Udovich and R.C. Edwards (to AMOCO) US Patent No. 4 564 688 (1986).
[4] B.J. Barone, Eur. Patent No. 458541 (assigned to Scientific Design Co.), US Patent No. 5 070 060 (1981).
[5] R.A. Schneider (to Chevron) US Patent No. 4 043 943 (1977).
[6] J.R. Ebner (assigned to Monsanto Co.), US Patent No. 185 455 (1933).

[7] J.X. Mc. Dermott (assigned to Halcon Co.), Ger. Offen No. 2 834 554 (1979).
[8] B.J. Barone (assigned to Scientific Design Co.) US Patent, 5 158 923 (1992).
[9] B.K. Hodnett, Catal. Today, 1 (1987) 477.
[10] E. Bordes, Catal. Today, 1 (1977) 499.
[11] F. Ben Abdelouahab, R. Olier, N. Guilhaume, F. Lefebvre and J.C. Volta, J. Catal., 134 (1992) 151.
[12] M. Abon, K.E. Bere, A. Tuel and P. Delichére, J. Catal., 156 (1995) 28.
[13] G. Centi, Catal. Today, 16 (1993) 5.
[14] F. Garbassi, J. Bart, R. Tassinari, G. Vlaic and P. Labarde, J. Catal., 98 (1986) 317.
[15] L.M. Cornaglia, C. Caspani and E. Lombardo, Appl. Catal., 74 (1991) 15.
[16] J. Li, M.E. Lashier, G.L. Schrader and B.C. Gerstein, Appl. Catal., 74 (1994) 15.
[17] M.T. Sananés, A. Tuel and J.C. Volta, J. Catal., 145 (1994) 251.
[18] M.T. Sananés, A. Tuel, G.J. Hutchings and J.C. Volta, J. Catal., 148 (1994) 395.
[19] M.T. Sananés, G.J. Hutchings and J.C. Volta, J. Catal., 154 (1995) 253.
[20] G.J. Hutchings, R. Olier, M.T. Sananés and J.C. Volta, Stud. Surf. Sci. Catal., 82 (1994) 213.